Horizontal Convection in an Enclosure with Fixed and Moving Walls

K. Y. Wong[1]**, M. P. King**[1] **and G. J. Sheard**[2]

[1] School of Engineering, Monash University, Sunway, Selangor D.E. 46150, Malaysia

[2] Department of Mechanical and Aerospace Engineering, Monash University, Victoria 3800, Australia

Abstract

Horizontal convection refers to the flow driven by a buoyancy imbalance along a horizontal level. In this study, two-dimensional simulations of horizontal convection in a rectangular enclosure are performed. Continuing from a previous study of horizontal convection in an enclosure with stationary walls, this paper considers an enclosure with movement applied to the floor, upon which the buoyancy imbalance is applied. This moving boundary provides mechanical stirring to the convective circulation in the enclosure. Our results identify both a forced convection regime driven by shear on the moving wall; and beyond a transitional Rayleigh number, a free convection regime driven by the temperature gradient on the heated boundary. We also report on the scaling correlations for Nusselt number in terms of the controlling parameter, Rayleigh number.

Introduction

In the extensively studied problems of confined free convection, such as the Rayleigh-Bénard convection, the thermal forcings are applied to more than one surface. For horizontal convection, the thermal forcing (either by a temperature gradient or a variation in heat flux) is applied along one horizontal boundary, while the other boundaries are usually thermally insulated.

Horizontal convection is commonly used as an idealised model to study the fluid dynamics and heat transfer in the meridional overturning circulations (MOC) of the oceans. It may also have applications in geological flows, engineering heat transfer and built-environment indoor climate.

A relatively thin top layer of the ocean is heated differentially from the equatorial to the polar regions. An important scientific question is that whether the observed MOC is primarily a heat engine (i.e. driven by the horizontal convection) or that it is driven mechanically, for example by winds and internal tides. The dominant current understanding supports the latter (see the review by Wunsch and Ferrari [9]); although other researchers have carried out studies which indicate that horizontal convection should not be ignored (e.g. Mullarney *et al.* [4]; Hughes and Griffiths [3]).

In Sheard and King [6], numerical investigations were performed with an in-house computational fluid dynamics (CFD) code. In that study the model was a two-dimensional rectangular enclosure of various aspect ratios, with an applied temperature gradient along the bottom wall (referred to here as the floor) and other walls being thermally insulted. It was determined that for an intermediate range of Rayleigh numbers (approximately $10^4 \lesssim Ra \lesssim 10^9$) where steady convective flows dominate, the Nusselt number, boundary layer thicknesses and peak boundary layer velocity scale with the Rayleigh number by exponents with values of $1/5$, $-1/5$, and $2/5$, respectively. These results were in agreement with established theory [5, 4, 3], and the relationships were independent of the enclosure aspect ratio.

A significant result arising from Sheard and King [6] is that unsteady flow develops above a critical Rayleigh number of
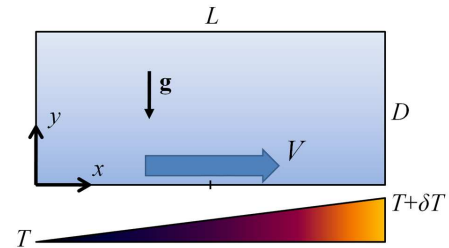

Figure 1: A schematic diagram of the system. The origin of the coordinate system is positioned at the bottom-left corner, gravity acts vertically downward, and a temperature difference of δT is imposed along the bottom wall, which is moving with a velocity V.

somewhere between 3.5×10^8 and 8.5×10^8. The onset of unsteadiness was detected by examining the time dependency of the heat fluxes through the floor. The unsteadiness in the flow is found mainly in the plume region due to entrainment, and eddies which are caused by the returning flow out of the plume at the top of the tank.

In the current study, we introduce an additional driver to the flow in the enclosure. Here, the floor is moving at a constant speed (as in the lid-driven cavity flow) in a direction which aids the existing convective circulation due to horizontal convection alone. This may model the effect of winds which provide kinetic energy to the oceans. Necessarily, our approach is an oversimplification because, among other reasons, the winds and the sea-surface temperature in the real oceans are coupled effects rather than independently prescribed. However, it is appropriate here as an additional complexity is being introduced to what is already a highly idealised model. It is also an interesting combination of a rather widely studied horizontal convection problem and the classical lid-driven cavity flow (Ghia *et al.* [2]).

Numerical model

Problem definition

The model considered here to study horizontal convection with a moving floor comprises a two-dimensional rectangular fluid-filled enclosure of width L and height D. The system is depicted in figure 1. The aspect ratio of the enclosure is defined as AR $= D/L$.

The flow is driven by both a linear temperature profile applied along the floor, as well as a uni-directional constant-speed linear motion of the floor. Relative to the enclosure, the temperature profile along the floor is unchanged, despite the floor moving in one direction (it is not clear how these conditions might be realised in the laboratory, but numerical implementation is straightforward). Zero-velocity (no-slip) conditions are imposed on the side and top walls, which are also thermally insulated by imposition of a zero outward normal temperature gradient.

Governing equations and dimensionless parameters

The dimensionless governing equations include momentum, mass conservation, and temperature transport equations. Respectively, these are written as

$$\frac{\partial \mathbf{u}}{\partial t} = -\left(\mathbf{u} \cdot \nabla\right)\mathbf{u} - \nabla p + Pr\,\nabla^2 \mathbf{u} - Pr\,Ra\,\hat{\mathbf{g}}T, \tag{1}$$

$$\nabla \cdot \mathbf{u} = 0, \tag{2}$$

$$\frac{\partial T}{\partial t} = -\left(\mathbf{u} \cdot \nabla\right)T + \nabla^2 T, \tag{3}$$

where $\mathbf{u}$ is the velocity vector, p the kinematic static pressure, t is time, Ra is the Rayleigh number, Pr the Prandtl number, $\hat{\mathbf{g}}$ the unit vector in the direction of gravity, and T is temperature. Here, lengths are scaled by L, velocities by κ_T/L (where κ_T is the thermal diffusivity), time by L^2/κ_T, and temperature by δT.

A Boussinesq approximation for the fluid buoyancy is used, whereby density differences in the fluid are neglected except in the gravity term (the term containing Ra in equation 1).

The horizontal Rayleigh number is defined as

$$Ra = \frac{g\alpha\delta T L^3}{\nu\kappa_T},$$

where g is the gravitational acceleration, ν the kinematic viscosity, and α the volumetric expansion coefficient of the fluid. The Prandtl number of the fluid is

$$Pr = \frac{\nu}{\kappa_T},$$

and in this study Pr is fixed at 6 (consistent with water). The Nusselt number, a measure of the ratio of convective to conductive heat transfer, is

$$Nu = \frac{F_T L}{\rho c_p \kappa_T \delta T},$$

where the heat flux is

$$F_T = \kappa_T \rho c_p \overline{\frac{\partial T}{\partial y}}.$$

In these relations, ρ is the reference density, c_p the specific heat capacity of the fluid, and $\overline{\frac{\partial T}{\partial y}}$ the average absolute vertical temperature gradient along the floor. Finally, a Reynolds number for the moving floor with velocity V is
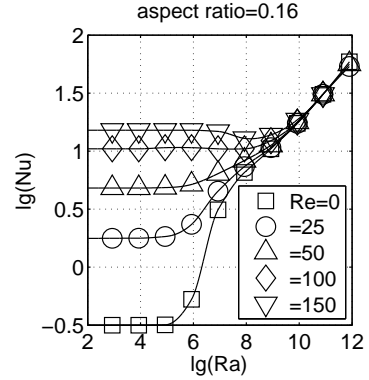
$$Re = \frac{VL}{\nu},$$

where a zero Reynolds number corresponds to conventional horizontal convection.

Numerical method

The governing equations are solved along with the stated boundary conditions on a two-dimensional domain using an in-house code employing spectral-element spatial discretisation (with a polynomial of degree 8 on each element) and a third-order time integration scheme based on backward differencing. The meshes and algorithm are the same as those used in [6]. Mesh resolution is concentrated in the vicinity of the walls, particularly adjacent to the heated floor. These meshes feature a higher resolution than has been employed in earlier studies (see [6] for further details).
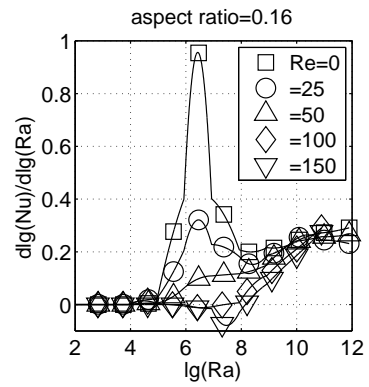
(a)

(b)

Figure 2: Horizontal convection in an enclosure with AR $= 0.16$ with a moving floor. (a) A plot of $\log(Nu)$ against $\log(Ra)$ for various Re. Akima splines are fitted to the data. (b) Gradients of the data in (a); i.e. showing γ-variation in the $Nu \sim Ra^\gamma$ relationships.

The code has been validated and employed on a wide range of studies (e.g. [7, 1, 6]). Additionally, relevant to the setup for the present study, validations were carried out against two studies: lid-driven flow in a square cavity [2], and horizontal convection at $Ra \approx 10^{12}$ for an enclosure with AR $= 0.16$ [4]. In each case a good agreement was obtained between the present algorithm and results reported in those studies.

Results and discussion

Heat transfer (Nu) scaling correlations

Heat transfer through the floor is considered at aspect ratios AR $= 0.16$ and 1. For these enclosures, computed Nusselt numbers are plotted against the Rayleigh number in figures 2a and 3a. In figures 2b and 3b, log-log gradients corresponding to values of γ in the $Nu \sim Ra^\gamma$ relationships are shown. Results are shown for a range of Reynolds numbers. Two main observations can be made about these results:

Firstly, for the parameters considered in this study, above $Ra \approx 10^9$, all of the Nusselt-number correlation curves converge to the curve for $Re = 0$, where the Nu–Ra relationships are independent of Reynolds number, but instead are dependent on the Rayleigh number. The transitional Rayleigh number ($Ra \approx 10^9$) delineates forced-convection and free-convection regimes. The transition Rayleigh number for the onset of unsteady horizontal convection flow is also found to be $Ra \approx 10^9$ [6].

Secondly, in agreement with theory, $\gamma = 0.2$ is observed over a range of Rayleigh numbers. This is especially clear for the
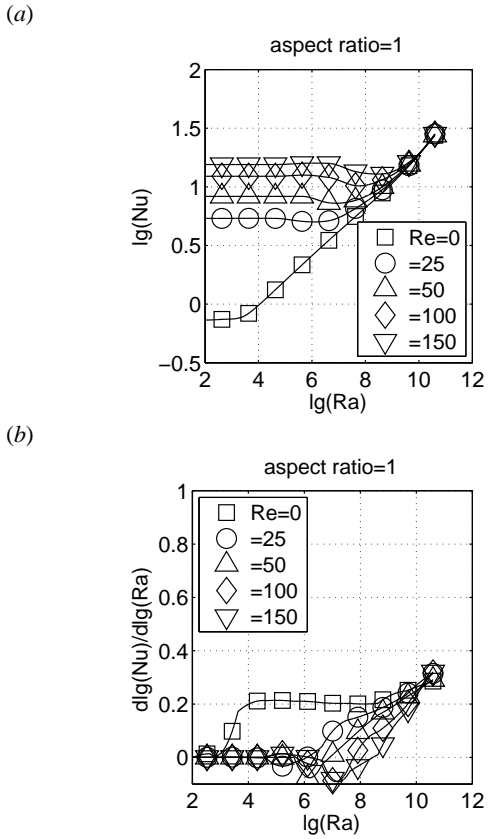
Figure 3: Horizontal convection in an enclosure with AR = 1 with a moving floor. (*a*) and (*b*) are as per figure 2.

$Re = 0$ cases (also reported in [6]). Significantly, here we also observe the further evidence of γ values approaching 0.3 at higher Rayleigh numbers (see figures 2*b* and 3*b*). Siggers *et al.* [8] derived an upper-bound of $\gamma = 1/3$ using the method of variational calculus. As far as we are aware, the current study and [6] are the first numerical or laboratory studies of horizontal convection to observe a trend approaching the upper-bound value. Generally the $\gamma = 1/5$ trend was observed in previous studies [5, 4, 8, 3].

The effect of an increase in γ on heat transport in the real oceans can be estimated by an order-of-magnitude calculation [8]. Using $L = 10^7$ m, $\alpha = 10^{-5}$ K^{-1}, $\delta T = 10$ K, $g = 10$ m s^{-2}, $\nu = 10^{-6}$ m^2 s^{-1}, $\kappa_T = 10^{-7}$ m^2 s^{-1}, we have an oceanic $Ra = 10^{31}$. With $Nu = 0.1Ra^{0.2}$ from our simulated data (figures 2 and 3), and using $\rho = 10^3$ kg m^{-3}, $c_p = 4200$ J kg^{-1} K^{-1}, and an area of 10^{12} m^2, we obtain $F = 6.6 \times 10^{10}$ W (by comparison, Siggers *et al.* [8] estimated $F = O(10^{11})$ W). This estimate is very small compared to $O(10^{15})$ W for poleward oceanic heat transport. However, for $\gamma = 0.3$ we obtain $F = 8 \times 10^{13}$ W, and for $\gamma = 1/3$ we have $F = 9 \times 10^{14}$ W, which are comparable to the oceanic value. This type of calculation is imprecise (not least as Nu is calculated by extrapolation) and is not useful for deciding whether the MOC is a buoyancy-induced flow caused by horizontal convection (a heat engine) or that horizontal convection plays a minor role while winds and internal tides are more important drivers. Nevertheless, the estimates calculated here suggest that for high-Rayleigh-number unsteady horizontal convection, the amount of heat transported can be 3 to 4 orders of magnitude higher than previously thought.

Some qualitative flow structures

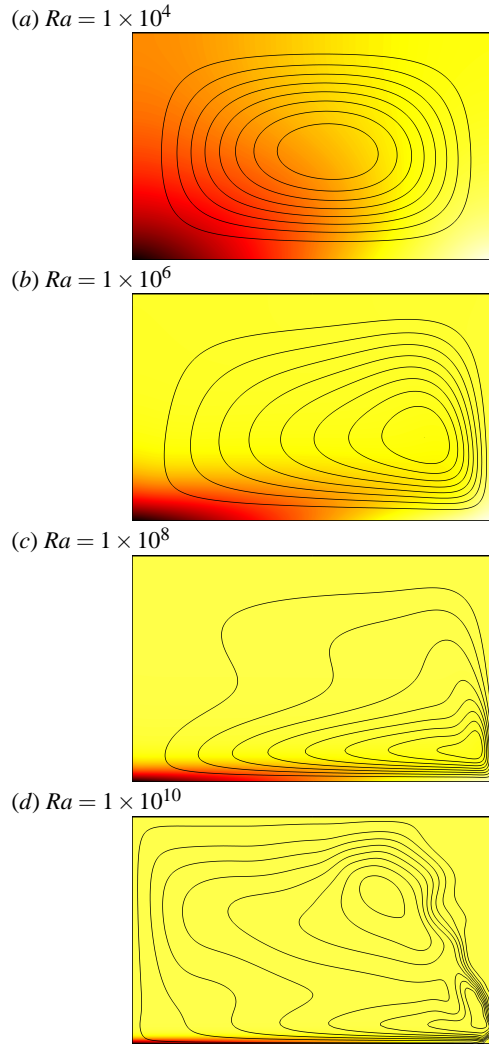A single convective circulation is observed in horizontal con-

Figure 4: Horizontal convection at various Rayleigh numbers in an enclosure with AR = 0.625 visualized using flooded temperature contours overlaid with streamlines. Dark (cold) to light (hot) contours show a temperature range of δT, and streamlines are equi-spaced between the minimum and maximum value of the streamfunction in each frame.

vection [5, 4, 3, 6]. Near the floor, a boundary layer is established, and flow moves towards the heated end, where it rises as a plume. At the top of the plume, there is a returning flow. Mixing due to the returning flow and diffusion cause the flow to lose buoyancy and complete the circulation. Figure 4 shows the effect of Rayleigh number on horizontal convection without a moving floor. In figure 4*a*, diffusion dominates; in figure 4*b-c*, convective effects become increasingly more pronounced; and in figure 4*d*, boundary-layer instability leads to a time-varying feeding of buoyancy into the plume. Figure 5 shows the vicinity of the plume at Rayleigh numbers across the threshold for unsteady flow in the enclosure [6]. As Rayleigh number is increased, the scale of structures within the plume is seen to decrease in accordance with theory. Figure 4*c* shows the formation of a mushroom-shaped packet of buoyant fluid in the boundary layer to the left of the plume, which demonstrates that instability in the boundary layer must be the source of time-dependence in this flow.

As mentioned earlier, for horizontal convection with a moving floor, a transition from forced convection to free convection is observed. The implication for this on the flow structure is
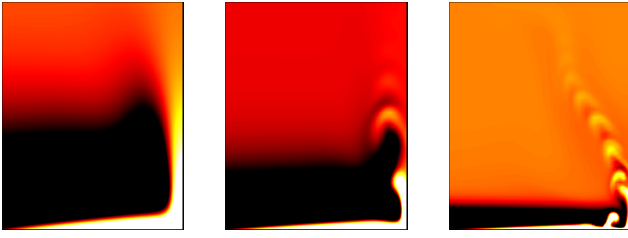
Figure 5: Detail view of the bottom-right-hand corner of an enclosure with AR = 0.625 at Rayleigh numbers $Ra = 1 \times 10^8$ (left), 1×10^9 (middle) and 1×10^{10} (right). Dark to light shading shows variation over a narrow range of temperatures arbitrarily chosen to visualize structures within the plume.
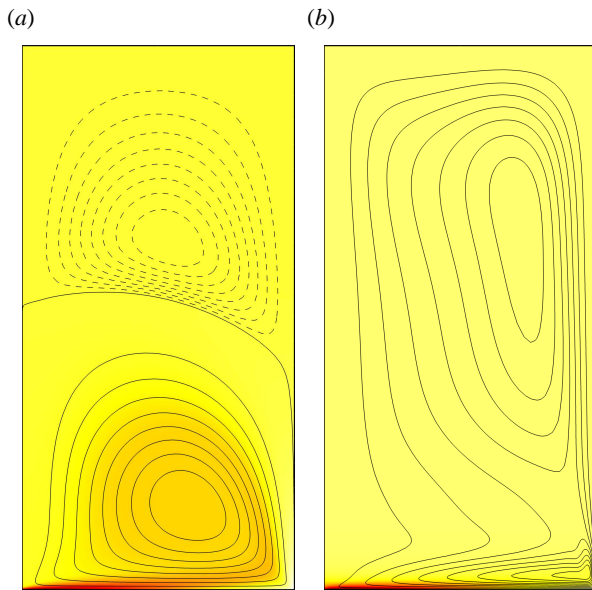

Figure 6: Plots of temperature and streamlines for horizontal convection in an enclosure with AR = 2 and a moving floor giving $Re = 150$. The temperature profile along the floor increases to the right, and the floor is moving to the right. Rayleigh numbers (a) $Ra = 100$ and (b) 10^8 are shown. Temperature contours are as per figure 4. Solid streamlines show counter-clockwise circulation, and dashed streamlines show clockwise circulation. In (a), the secondary (clockwise) circulation is approximately 2% of the strength of the primary circulation.

that the double circulations which exist in the forced convection regime under some conditions (for certain aspect ratios and Re, as in the lid-driven cavity flow) would revert to a single convective circulation as Rayleigh number is increased and the flow shifts to the free-convection regime (dominated by horizontal convection).

An example of this behaviour is demonstrated in figure 6, which shows streamlines obtained at a fixed Reynolds number and aspect ratio, for flows with $Ra = 100$ (forced convection) and $Ra = 10^8$ (free convection).

Conclusions

Horizontal convection with a moving floor in a two-dimensional rectangular enclosure is investigated using an in-house CFD code employing the spectral element method. It is found that a transitional Rayleigh number ($Ra \approx 10^9$) delineates a forced-convection and a free-convection regime. Examining the $Nu \sim Ra^\gamma$ relationships found $\gamma \approx 0.2$ for some intermediate Rayleigh numbers. Above $Ra \approx 10^9$, an increasing trend reaching $\gamma \approx 0.3$ was observed, perhaps approaching the theoretical upper bound of $\gamma = 1/3$. A previous study [6] found that the flow also becomes unsteady at around this Rayleigh number. The implication of this for the real oceans is that at high Rayleigh number $Ra = O(10^{31})$, the poleward heat transported by horizontal convection may be 3 to 4 orders of magnitude higher than previously thought (i.e. $O(10^{15})$ W as opposed to $O(10^{11})$ W).

References

[1] Blackburn, H. M. and Sheard, G. J., On quasi-periodic and subharmonic Floquet wake instabilities, *Phys. Fluids*, **22**, 2010, 031701.

[2] Ghia, U., Ghia, N. and Shin, C. T., High-Re solutions for incompressible flow using the Navier–Stokes equations and a multigrid method, *J. Comput. Phys.*, **48**, 1982, 387–411.

[3] Hughes, G. O. and Griffiths, R. W., Horizontal convection, *Annu. Rev. Fluid Mech.*, **40**, 2008, 185–208.

[4] Mullarney, J. C., Griffiths, R. W. and Hughes, G. O., Convection driven by differential heating at a horizontal boundary, *J. Fluid Mech.*, **516**, 2004, 181–209.

[5] Rossby, T., Numerical experiments with a fluid heated non-uniformly from below, *Tellus*, **50A**, 1998, 242–257.

[6] Sheard, G. J. and King, M. P., Horizontal convection: Effect of aspect ratio on Rayleigh-number scaling and stability, *Appl. Math. Mod. (In Press)*, doi:10.1016/j.apm.2010.09.041.

[7] Sheard, G. J., Leweke, T., Thompson, M. C. and Hourigan, K., Flow around an impulsively arrested circular cylinder, *Phys. Fluids*, **19**, 2007, 083601.

[8] Siggers, J. H., Kerswell, R. R. and Balmforth, N. J., Bounds on horizontal convection, *J. Fluid Mech.*, **517**, 2004, 55–70.

[9] Wunsch, C. and Ferrari, R., Vertical mixing, energy, and the general circulation of the oceans, *Annu. Rev. Fluid Mech.*, **36**, 2004, 281–314.